Marine Biotechnology (2020) 22:357–366
https://doi.org/10.1007/s10126-020-09955-6

ORIGINAL ARTICLE

Evaluation of the In Vivo Biological Effects of Marine Collagen and Hydroxyapatite Composite in a Tibial Bone Defect Model in Rats

Julia Risso Parisi[1] · Kelly Rossetti Fernandes[1] · Matheus de Almeida Cruz[2] · Ingrid Regina Avanzi[2] · Alan de França Santana[2] · Giovanna Caroline Aparecida do Vale[2] · Ana Laura Martins de Andrade[1] · Cíntia Pereira de Góes[2] · Carlos Alberto Fortulan[3] · Eliandra de Sousa Trichês[4] · Renata Neves Granito[2] · Ana Claudia Muniz Rennó[2]

Received: 2 July 2019 / Accepted: 4 February 2020 / Published online: 25 April 2020

Abstract

One of the most promising strategies to improve the biological performance of bone grafts is the combination of different biomaterials. In this context, the aim of this study was to evaluate the effects of the incorporation of marine spongin (SPG) into Hydroxyapatite (HA) for bone tissue engineering proposals. The hypothesis of the current study is that SPG into HA would improve the biocompatibility of material and would have a positive stimulus into bone formation. Thus, HA and HA/SPG materials were produced and scanning electron microscopy (SEM) analysis was performed to characterize the samples. Also, in order to evaluate the in vivo tissue response, samples were implanted into a tibial bone defect in rats. Histopathological, immunohistochemistry, and biomechanical analyses were performed after 2 and 6 weeks of implantation to investigate the effects of the material on bone repair. The histological analysis demonstrated that composite presented an accelerated material degradation and enhanced newly bone formation. Additionally, histomorphometry analysis showed higher values of %BV/TV and N.Ob/T.Ar for HA/SPG. Runx-2 immunolabeling was higher for the composite group and no difference was found for VEGF. Moreover, the biomechanical analysis demonstrated similar values for all groups. These results indicated the potential of SPG to be used as an additive to HA to improve the biological performance for bone regeneration applications. However, further long-term studies should be carried out to provide additional information regarding the material degradation and bone regeneration.

Keywords Marine biotechnology · Collagen · Spongin · Marine sponges

Introduction

The development of bone substitutes for critical skeletal bone defects that cannot heal has been the aim of investigation in the field of bone tissue engineering. These defects are common in clinical practice and are related to associated diseases, tumors, and extensive bone loss (Sarkar and Lee 2015; Guerado and Caso 2017). A series of bone graft materials to treat these affections have been extensively used such as autografts, allografts and synthetic bone substitutes (Matassi et al. 2011; Smith et al. 2011). Autologous bone grafts are considered the gold standard in the area of bone tissue engineering, but the need of an additional surgery and the amount of tissue available limited their use (Dimitriou et al. 2011; Mishra et al. 2016). Allografts, although their positive effects, have major associated limitations with risk of rejection and transmission of diseases (Oryan et al. 2014). In this context, synthetic bone substitutes, including mainly hydroxyapatite (HA), calcium phosphate

Electronic supplementary material The online version of this article (https://doi.org/10.1007/s10126-020-09955-6) contains supplementary material, which is available to authorized users.

✉ Julia Risso Parisi
juliaparisi@outlook.com

[1] Department of Physiotherapy, Federal University of São Carlos (UFSCar), Washington Luís, km 235, Sao Carlos, SP, Brazil

[2] Department of Biosciences, Federal University of São Paulo (UNIFESP), Santos, SP, Brazil

[3] Department of Mechanical Engineering, São Carlos School of Engineering, Sao Carlos, SP, Brazil

[4] Department of Mechanical Engineering, Federal University of São Paulo (UNIFESP), Sao Jose dos Campos, SP, Brazil

(CaP) ceramics (Dorozhkin 2010; Denry and Kuhn 2015), and polymer-based materials (Campana et al. 2014), have been developing trying to solve some of the problems cited above.

HA bone grafts are one of the most common materials used in the area of bone tissue engineering due to biocompatibility and osteoconductive properties (Bhatt and Rozental 2012; Wang and Yeung 2017). Although the effects of HA on bone tissue metabolism are stimulatory, the rate of HA degradation is too slow (avoiding its substitution by newly formed bone) and its capacity to stimulate bone metabolism and ingrowth is limited (Wang et al. 2007; Parizi et al. 2013; Pang et al. 2015).

Consequently, the association of the different materials, combining their diverse properties such as bioactivity and mechanical strength, possibly may constitute a bone graft with improved biological performance (Pang et al. 2015; Siddiqui et al. 2018). In this context, biomimetic grafts, with an inorganic part (HA for example) with an organic component (such as collagen), mimicking the structure and composition of bone tissue, may be an optimized treatment for improving bone healing (Pek et al. 2008; Gleeson et al. 2010; Walsh et al. 2019). As an example, Gleeson et al. (2010) developed a biomimetic scaffold by incorporating HA particles into a highly porous collagen-based scaffold, through suspension using a freeze-drying method. Similarly, Pek et al. (2008) developed a scaffold constituted by collagen and HA (manufactured by mixing physically all the components) and evidenced its positive effect on bone healing.

Besides, marine collagen (or spongin-SPG), extracted from sponges (Poriferas), is a very interesting alternative to be used for bone tissue engineering applications (Wang et al. 2009; Silva et al. 2014; Granito et al. 2017; Parisi et al. 2019). SPG consists of large structures formed by collagen microfilaments, glycoproteins, and proteoglycans (Junqua et al. 1974; Green et al. 2003; Iwatsubo et al. 2015; Pozzolini et al. 2018). It presents low risk of transmission of infection-causing agents and good biocompatibility and provides mechanical stability/integrity to tissues (Granito et al. 2017; Pozzolini et al. 2018).

A recent in vitro study demonstrated that SPG can successfully be introduced into HA and present a very positive effect on osteoblast and fibroblast proliferation (Parisi et al. 2019). The encouraging in vitro data on the association of SPG into HA composites formed the basis for this in vivo study, which aimed to evaluate the orthotopic in vivo response into HA/SPG samples. Composites that were implanted into tibial defects of rats and bone response (histology, histomorphometry, and immunohistochemistry) were evaluated after 2 and 6 weeks of implantation.

Materials and Methods

Materials

The main material used in this study was hydroxyapatite, containing calcium phosphate and hydroxyl ($Ca_{10}(PO_4)_6(OH)_2$), the density of this powder is 2.82 g/cm^3, and provided by the Science and Technology Institute-Universidade Federal de São Paulo (São José dos Campos, São Paulo, Brazil).

Aplysina fulva marine sponge was used for SPG extraction. Samples were collected in Praia Grande (São Sebastião, Brazil). SPG was extracted by the method bellow, based in a previously described method by Swatschek et al. (2002). The extraction procedure was entirely performed at 2 °C. Small pieces of this species of marine sponges were mixed with 100 mM Tris-HCl buffer (pH 9.5, 100 mM 2-mercaptoethanol, 8 M urea, 10 mM EDTA) and the pH was adjusted to 9 (NaOH solution). Solution was stirred for 24 h and centrifuged for 5 min (5000*g*; 2 °C), the supernatant removed, and the pH was adjusted to 4 (acetic acid solution). Additionally, the solution was centrifuged for 40 min (18,000*g*; 2 °C) and the precipitate was solubilized in Milli-Q water and centrifuged again during 40 min (18,000*g*; 2 °C). The solution was lyophilized and stored at room temperature.

Preparation of Scaffolds

For this study, scaffolds (100% for HA and 70% of HA and 30% of SPG for the composites) were manufactured using different materials following the protocol described in a previous study (Parisi et al. 2019). Poly (methyl methacrylate) (PMMA) with particle size 15 μm (VIPI, Pirassununga, São Paulo, Brazil) was used to aggregate all the materials. In addition, carboxymethyl cellulose (CMC), density 1.59 g/cm^3, was provided by Sigma (Missouri, USA) and it is used to produce pores into the samples (around 60%) (Lopez-Heredia et al. 2012; Haach et al. 2014; Sousa et al. 2019). All materials described above, in powder, were weighed and mixed at the different proportions corresponding to each group (Table 1). After that, distilled water and methyl methacrylate (MMA) with purity of 99.09% (VIPI, Pirassununga, São Paulo, Brazil) were inserted in the solution and mixed. Then, the mixture was transferred into a silicon mold (3 mm diameter × 2 mm height). After that, molds were sealed and pressurized at air chamber (at 0.6 MPa) for 30 min and vacuum dried (10^{-3} Torr) for 15 min. The composites were removed from the silicon molds and submitted to sterilization by ethylene oxide (Acecil, Campinas, SP, Brazil) according to Fernandes et al. (2019).

SEM Morphology

The morphology of the materials was analyzed by a scanning electron microscope (LeO 440, Carl Zeiss, Jena, Germany).

In Vivo Study

All animal experiments were performed in accordance with protocols approved by Experimental Animal Committee of

Table 1 Experimental groups with the different formulations of composites

Groups	PMMA (g)	MMA (g)	HA (g)	SPG (g)	CMC (g)	Water (g)
HA	0.236	0.472	0.564	0	0.043	0.565
HA/SPG	0.236	0.472	0.296	0.127	0.043	0.565

the Federal University of São Paulo (2017-1952071216) and national guidelines for the care and use of laboratory animals were strictly observed. Forty-eight male Wistar rats (12 weeks old and weighting 300 ± 350 g) were divided into three groups: control group (CG), hydroxyapatite group (HA), and hydroxyapatite and spongin group (HA/SPG). After surgery, each group was divided into two different euthanasia periods (2 and 6 weeks). The surgical procedure was the same for all the rats: it was induced that a noncritical bone defect to both tibia and this whole was filled with the different group materials. They were kept under controlled conditions (temperature 22 ± 2 °C, light–dark periods of 12 h, and free access to water and commercial diet).

Surgery Procedure

Surgical procedure was performed following the Magri et al. (2015) method. For the anesthesia, the following anesthetics were injected intraperitoneally: ketamine (80 mg/kg), xylazine (8 mg/kg), acepromazine (1 mg/kg), and fentanyl (0.05 mg/kg), all medications provided by Syntec (Santana de Parnaíba, São Paulo, Brazil). Then, a tibial defect was provided to every leg of the rat (3 mm diameter) using motorized drill (Beltec®, Araraquara, SP, Brazil). Under copious irrigation with saline solution, 10 mm distal of the knee joint of the tibia got an implant; those materials were placed in the created defect, according to each group ($n = 8$ per experimental group). After that, the wound was sutured with nylon (Shalon®, Alto da Boa Vista, PR, Brazil). Euthanasia was performed after 2 and 6 weeks post-surgery using CO_2 suffocation.

Histopathological Analysis

After euthanasia, the right tibias were removed and immediately fixed in 10% formalin (Merck, Darmstadt, Germany). After 2 days, the material was decalcified in 4% of ethylenediaminetetraacetic acid (EDTA) (Merck, Darmstadt, Germany) and dehydrated different concentrations of ethanol. For the block preparations, the dehydrated material was inserted into molds containing paraffin. Therefore, for the histopathological procedure, using a microtome with a blade (Leica Microsystems SP 1600, Nussloch, Germany), thin sections (4 μm) were performed and stained with hematoxylin and eosin (Merck, Darmstadt, Germany). The laminas were examined using light microscopy (Leica Microsystems AG, Wetzlar, Germany, Darmstadt-Germany). Presence of granulation tissue, newly formed bone, inflammatory process, and the presence of material were investigated per animal. The analysis was performed by two blinded observers (JRP and MAC).

Histomorphometric Analysis

Stained laminas were quantitatively scored by a Software called OsteoMeasure System (Osteometrics, Atlanta, GA, USA). Structural parameters were performed to inform the bone structure and volume of residual biomaterial into the defect. All samples were quantified separately for each specimen in order to compare between the experimental groups. The following parameters were analyzed for this procedure: osteoblast number per tissue area (N.Ob/T.Ar/mm^2), bone volume fraction (BV/TV, %), and percentage of bone surface occupied by osteoblast (Ob.S/BS) (Parfitt 1988). Two blinded experienced observers (JRP and GCAV) performed the analysis.

Immunohistochemistry Analysis

The protocol previously described by Fernandes et al. (2017) was used, using the streptavidin–biotin–peroxidase method for immunohistochemistry analysis. Concisely, xylene removed the paraffin from the sections, for that the laminas were dehydrated in different concentration of ethanol and pretreated with 0.01 M citric acid buffer (pH 6) for 5 min in a steamer. The endogenous peroxidase was inactivated using hydrogen peroxide in phosphate-buffered saline (PBS) for 5 min and blocked with 5% normal goat serum (Vector Laboratories, Burlingame, CA, USA) in PBS for 10 min. After that, anti-Runx-2 polyclonal (code: sc-8566, Santa Cruz Biotechnology, USA) at a concentration of 1:100 and VEGF monoclonal (code: sc-7269, Santa Cruz Biotechnology, USA) at a concentration of 1:100 were incubated overnight at 4 °C. Then, the concentration of 1:200 biotin-conjugated secondary antibody anti-rabbit IgG was used (Vector Laboratories, Burlingame, CA, USA) in PBS for 1 h. After that, the sections were washed PBS and were incubated with avidin biotin complex conjugated to peroxidase (Vector Laboratories) for 45 min. For immunostaining, 0.05% solution of 3-3′-diaminobenzidine solution was used and restrained with Harris hematoxylin (Merck) for 10 s. At the end, for the qualitatively analysis, the presence and location of the immunomarkers and semi-quantitative analysis were assessed using a light microscopy (Leica Microsystems AG, Wetzlar, Germany). According to a previously described scoring scale from 1 to 4 (1 = absent (0% of immunostaining),

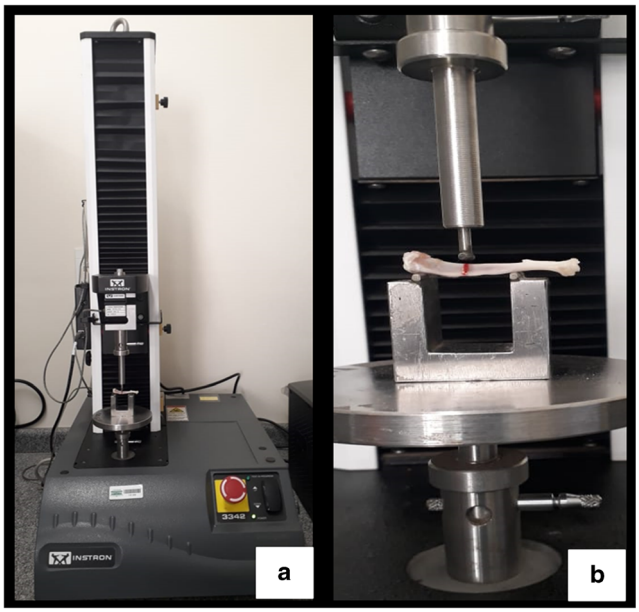

Fig. 1 This figure shows how the biomechanical test was performed: **a** Instron® Universal Testing Machine, 3342 model used in experiment. **b** The tibial position during the test

2 = weak (1–35% of immunostaining), 3 = moderate (36–67% of immunostaining), and 4 = intense (68–100% of immunostaining)) (Fernandes et al. 2017), two blinded experienced observers (JRP and GCAV) performed the analysis.

Biomechanical Test

A three-point bending test in an Instron® Universal Testing Machine (Instron® Worldwide Headquarters, Norwood, MA, USA), 3342 model and 500 N load cell was used for the mechanical test. The left tibiae were placed onto a device measuring 3.8 cm, providing a 1.8 cm distant double support on the diaphysis (Fig. 1). At the middle point of the tibiae, the load cell was vertically positioned. Firstly, a pre-load of 5 N was applied and the bending force at 0.5 cm/min constant deformation rate until the bone fracture. Finally, the software program calculates a load-deformation curve, the maximum load (N), and resilience (J) (Magri et al. 2015).

Statistical Analysis

Statistical analyses were performed using GraphPad Prism 6 Software (GraphPad Software, San Diego, CA, USA). All the data were expressed as mean ± standard deviation (SD). Distribution could be tested by Shapiro-Wilk normality test. For non-parametric data, Kruskal-Wallis test and Dunn post hoc were used. For parametric data, ANOVA (one-way analysis of variance) and Tukey multiple comparison post-tests were used. Significant differences at $p \leq 0.05$ were considered.

Results

Scaffold Morphology

Figure 2 demonstrates SEM representative micrographs for all experimental groups. For HA powder, granules were irregular and presented a smooth surface (Fig. 2a). Moreover, Fig. 2c demonstrated the fibers of SPG (Fig. 2b). In the HA scaffolds,

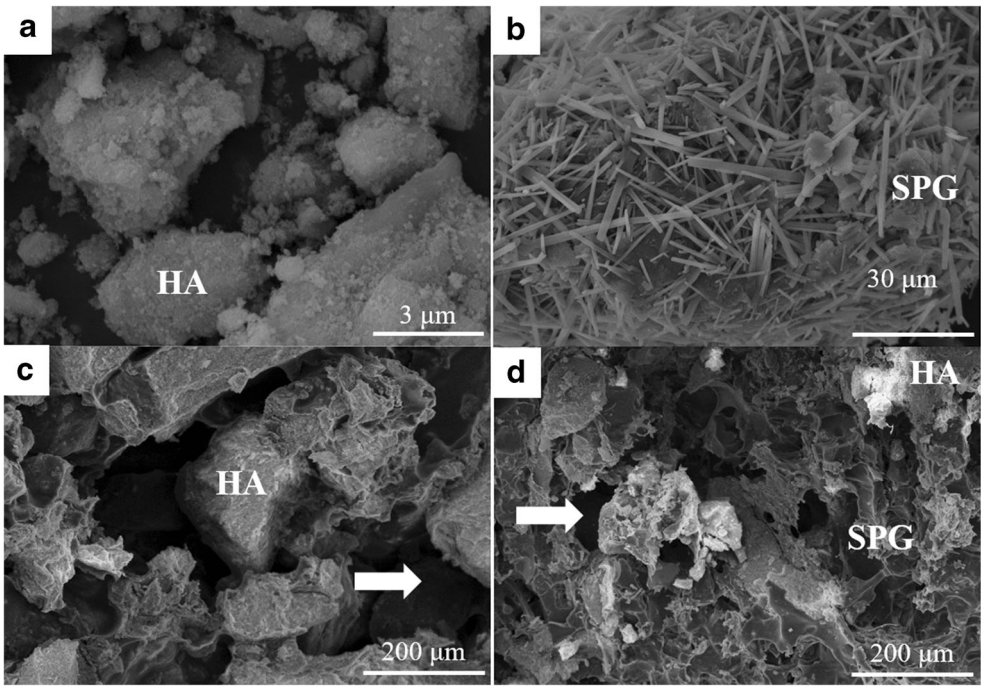

Fig. 2 Microscopic SEM micrographs. **a** HA powder form, scale bar = 3 µm. **b** SPG powder form (**b**), scale bar = 30 µm. **c** Scaffold of HA, scale bar = 200 µm. **d** Scaffold of HA/SPG pores (arrow), scale bar = 200 µm

particles of HA could be observed, with the presence of some pores (Fig. 2c). SEM images of HA/SPG demonstrated the presence of HA particles and fibers of SPG with presence of pores (Fig. 2d).

Descriptive Histopathological Analysis

Representative histological sections of all experimental groups, 2 and 6 weeks post-surgery, are shown in Fig. 3. Two weeks post-surgery, for CG, it is possible to observe granulation tissue at the center of the defect, which was also noticed, newly formed bone formation mainly at the edge of the defect (Fig. 3a). For HA, residual material could be observed, surrounded by granulation tissue, with some areas of newly formed bone at the borders of the defect (Fig. 3c). For HA/SPG, at the center of the defect, it is possible to observe residual material with some areas of granulation tissue. Additionally, an intense presence of newly formed bone in the edges of the defect was observed (Fig. 3e).

Six weeks post-surgery, for CG, it is possible to observe the formation of mature bone formation and granulation tissue (Fig. 3b). For HA, it is possible to observe complete degradation of the material with consequent formation of granulation tissue at the center of the defect and formation of mature bone at the edges of the lesion (Fig. 3d). For HA/SPG, a complete material degradation was observed, with the ingrowth of granulation tissue in the center of the defect. In addition, the edges were completely filled with newly formed bone (Fig. 3f).

Histomorphometric Analysis

A higher value of % BV/TV was found for CG and HA/SPG compared to HA, in both experimental periods ($p = 0.0113$, $p = 0.0487$, $p = 0.0401$, and $p = 0.0141$, respectively) (Fig. 4a).

Figure 4 b demonstrates that, for Ob.S/BS, a significantly higher value ($p = 0.0085$) was found for HA/SPG compared to HA, after 2 weeks. After 6 weeks, it is possible to verify a higher value ($p = 0.0184$) of Ob.S/BS for HA/SPG compared to CG. In addition, for N.Ob/T.Ar, no difference was found among groups (Fig. 4c).

Immunohistochemistry

Runx-2

After 2 and 6 weeks post-surgery, all experimental groups presented positive Runx-2 immunolabeling (Fig. 5).

All groups demonstrated Runx-2 immunolabeling predominantly in the granulation tissue after 2 weeks post-surgery. Additionally, 6 weeks post-surgery, in all groups, it was possible to observe a Runx-2 immunostaining in the granulation tissue and in the newly formed bone (Fig. 5b, d, f).

Figure 6 shows the results of the semi-quantitative analysis of Runx2 immunoexpression. In both periods analyzed (2 and 6 weeks), HA/SPG showed a significantly higher immunolabeling of Runx-2 expression compared to CG ($p = 0.005$).

VEGF

Figure 7 demonstrates the qualitative analysis of VEGF immunostaining after 2 and 6 weeks post-surgery. At 2 weeks, all groups showed a similar pattern of immunoexpression of VEGF, with the presence of VEGF marker in the granulation tissue (Fig. 7a, c, e). Furthermore, after 6 weeks, it is possible to observe that VEGF immunolabeling continues in the granulation tissue mainly at the center of the defect (Fig. 7b, d, f).

Figure 8 presents the semi-quantitative analysis of VEGF immunostainig after 2 and 6 weeks post-surgery. No significant difference was observed among the other groups in both periods analyzed of VEGF immunoexpression.

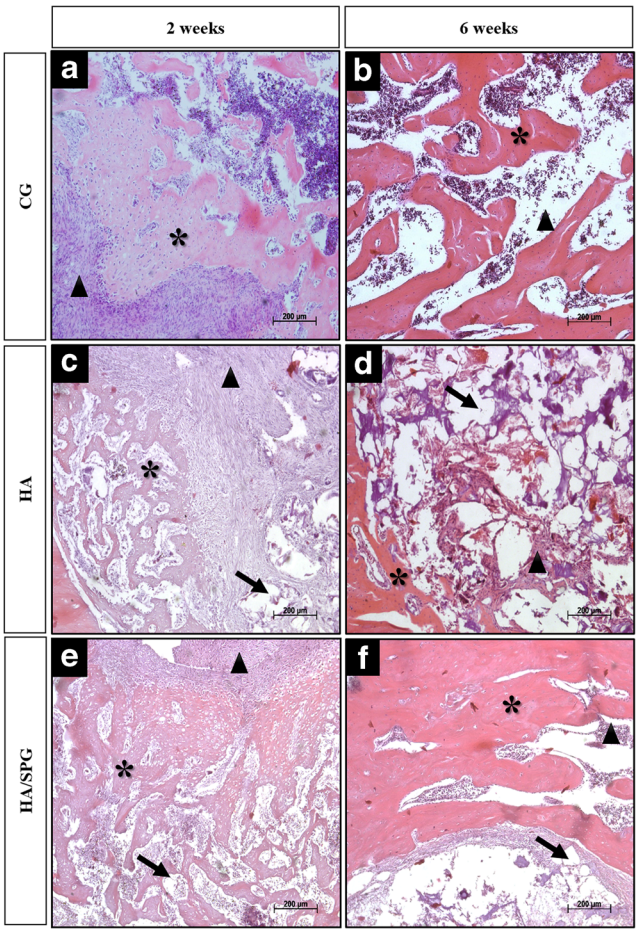

Fig. 3 Representative histological sections of tibial bone defects of the groups: control (**a**, **b**); HA (**c**, **d**); HA/SPG (**e**, **f**) after 2 and 6 weeks, respectively. Newly formed bone (*), granulation tissue (triangle), residual material (black arrow). Bar represents 200 μm (mag. × 2.5). Hematoxylin and eosin stain

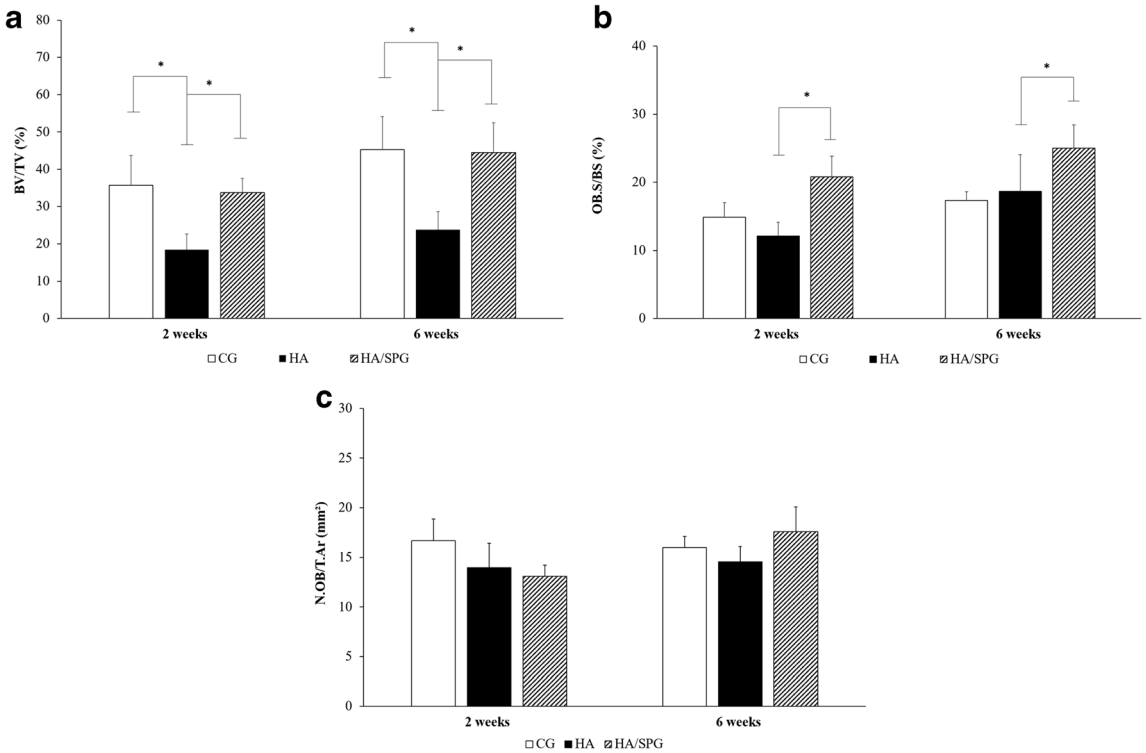

Fig. 4 Means and standard deviation of % of BV/TV, % of OB.S/BS, and N.Ob/T.Ar (mm^2). Dunn's test. $*p < 0.05$

Biomechanical Test

The biomechanical analysis showed value of the biomechanical test for maximun load (N), resilience (N/mm^2), and tenacity (J) (Table 2). No statistically significant difference was observed among groups for the parameters analyzed in both experimental periods (2 and 6 weeks post-surgery).

Discussion

This study aimed to evaluate the effects of HA/SPG composite using a model of implantation into tibial bone defects in rats after 2 and 6 weeks. It was hypothesized that SPG into HA would improve the biological performance of the composite and would have a positive stimulus into bone formation. The main histological findings demonstrated that the HA/SPG-treated animals presented an accelerated material degradation and enhanced newly bone formation. Moreover, histomorphometry analysis showed higher values of %BV/TV and N.Ob/T.Ar for HA/SPG. Runx-2 immunolabeling was higher for the composite group and no difference was found for VEGF. No statistical differences in the biomechanical analysis were observed between any groups.

It is well known that Col has a fundamental role in providing structural integrity to tissues, and due to its low immunogenicity and biocompatibility, it is an excellent biomaterial to be used for tissue engineering and regenerative medicine strategies in human health issues (Pozzolini et al. 2018). In this context, marine sponge is one of the most promising sources of Col for biomedical applications (Silva et al. 2014).

SEM analysis demonstrated that SPG could successfully be introduced into HA, forming a homogeneous scaffold. It is important to emphasize that the composition of the samples was chosen based on the percentages of organic and inorganic parts of bone mimic bone composition (Liu et al. 2017).

In this present study, histological analysis showed that HA/SPG composites revealed biocompatibility, with no signs of inflammatory reactions, confirming the results of other works in bone healing in maxillofacial (Thorwarth et al. 2005) and defects in long bones (Brandt et al. 2010). Also, the degradation behavior of the composites demonstrated a lower amount of remaining material and a higher amout of newly formed bone into the deffect area. HA is one of the most common biomaterial used for bone graft manufacturing mainly due to its biocompatibility and osteoconductive properties (Cassino et al. 2018). However, HA is characterized by a very slow degradation rate and low bioactivity index, which is considered as a disadvantage for several applications such as sinus elevation (Raucci et al. 2015). In this context, to enhance the osteogenic potential of HA, a colagenic part was introduced with the aim of increasing bone mineralization and tissue ingrowth (Scarano et al. 2017). The positive effects observed in the present study corroborate those of Alt et al. (2016) who demonstrated that HA/col-1 composites produced an increased index of

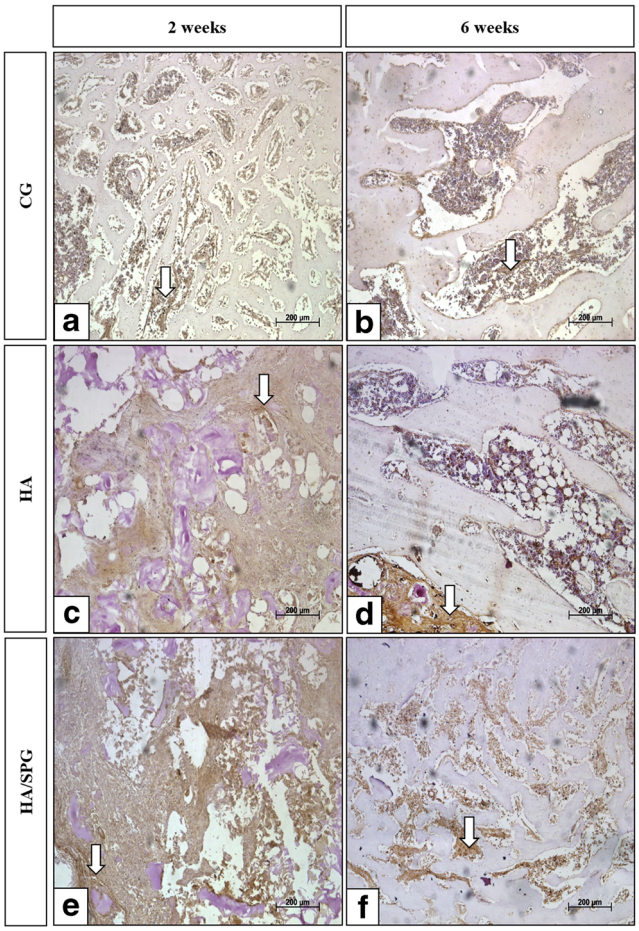

Fig. 5 Immunohistochemistry of Runx-2 for the experimental groups: control, HA, and HA/SPG after 2 and 6 weeks post-surgery. Runx-2 immunostaining (white arrow). Scale bar: 200 μm (mag. × 10)

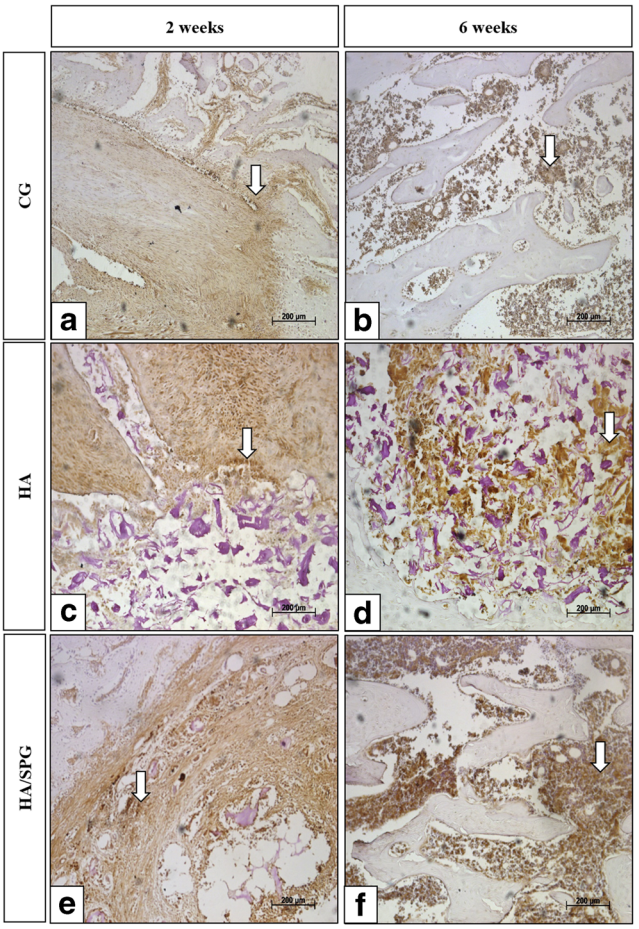

Fig. 7 Immunohistochemistry of VEGF for control, HA, and HA/SPG groups after 2 and 6 weeks post-surgery. VEGF immunostaining (white arrow). Scale bar: 200 μm (mag. × 10)

connectivity density and higher number of trabeculaes in osteoporotic metaphyseal bone defects in goats. It is likely that the superior biological performance of HA supplemented with Col is determined by the biomimetic composition of the grafts. It is well known that Col presents excellent biological features and physicochemical properties, being responsible by enhancing bone cell activity, and consequently increase bone deposition and mineralization, constituting a

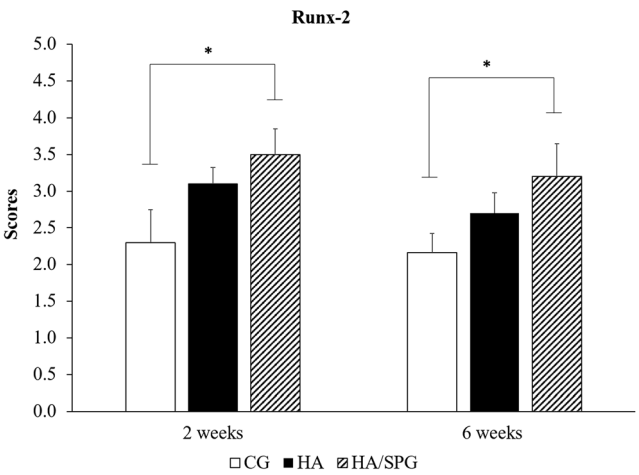

Fig. 6 Scores (mean ± SD) for immunoexpression of Runx-2 for the different experimental groups after 2 and 6 weeks post-surgery. Dunn's test. $*p < 0.05$

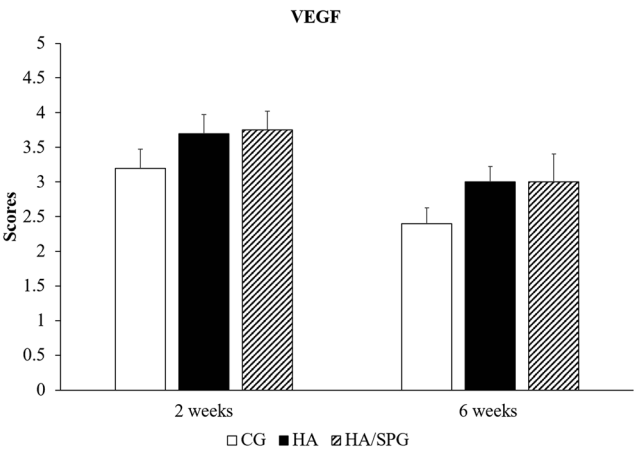

Fig. 8 Scores (mean ± SD) for immunoexpression of VEGF for the different experimental groups after 2 and 6 weeks post-surgery. Dunn's test. $*p < 0.05$

Table 2 Biomechanical evaluation parameters (mean ± standard error) of the rats tibias

	2 weeks			6 weeks		
	CG	HA	HA/SPG	CG	HA	HA/SPG
Maximal load (N)	53.43 ± 4.40	54.47 ± 6.84	62.76 ± 7.08	86.48 ± 3.369	76.81 ± 14.62	79.09 ± 11.90
Resilience (N/mm^2)	0.018 ± 0.0089	0.014 ± 0.0058	0.019 ± 0.0064	0.0310 ± 0.005	0.0236 ± 0.0069	0.0260 ± 0.0071
Tenacity (J)	0.03 ± 0.017	0.02 ± 0.020	0.02 ± 0.012	0.05 ± 0.02	0.03 ± 0.01	0.03 ± 0.01

very suitable material to be used as bone grafts (Lin et al. 2018; Zhang et al. 2018).

Concerning the immunohistochemistry analysis, difference in Runx-2 immunolabeling was observed for composite-treated animals (for both experimental periods). It is widely known that Runx-2 is essential for bone cell stimulation and regulation of the expression of many extracellular matrix protein genes during bone cell differentiation (Komori 2017; Wei et al. 2018). It may be suggested that the composites used in this study could have stimulated an earlier differentiation of pre-osteoblasts into mature osteoblasts, which consequently have led to an increased amount of newly formed bone deposition in HA/SPG.

Also, VEGF is a signal protein produced by cells that stimulate the formation of blood vessels and neoangiogenesis, which is an essential factor for an adequate healing. Interestingly, no difference was observed in VEGF immunolabeling among groups, indicating that HA/SPG composites did not have any extra effect on this immunomarker.

Furthermore, similar findings for biomechanical analysis were found for the experimental groups. This fact probably indicates that the groups presented analogous spatial distribution of the materials and/or the granulation tissue or newly formed bone, which culminate in the same bone strength. It may be suggested that in long-term periods after material implantation, differences would be observed, especially related to the higher amount of bone of HA/SPG animals. These data corroborate those of Wei et al. (2018) who found no difference in the callus biomechanical strength in HA/Col-treated animals using a model of rat femur osteotomy.

It is worthwhile to emphasize that this study was performed for a short-term evaluation after material implantation. In this context, the long-term biological performance of BS/SPG composites needs to be clarified. Also, it is necessary to investigate the effects of the present materials using a critical bone defect model to evaluate the behavior of composites in the process of non-spontaneous healing. Following this line, further investigations are necessary in order to validate these combinations as safe and efficient materials for biomedical applications.

Conclusions

As a conclusion, it was demonstrated that the addition of SPG into HA presents a promising strategy for stimulation bone healing and newly formed bone deposition, with a higher Runx2 imunolabeling. Interestingly, no differences were observed for VEGF imunolabeling and biomechanical analysis between the experimental groups. Consequently, these data highlight the potential of marine collagen (SPG) to be used as an additive to HA to improve the biological performance for bone regeneration applications. However, further long-term studies should be carried out to provide additional information concerning the late stages of material degradation and bone regeneration induced by the composites. Also, it would be interesting to evaluate the biological performance of Ha/SPG composites in compromised situations.

Acknowledgments The authors would like to acknowledge CAPES Foundation, Ministry of Education of Brazil, Brasilia-DF, Brazil. Prof. Dr. Márcio Reis Custódio from Department of General Physiology of the Institute of Biosciences (IB-USP) for the assistance with this experiment.

Compliance with Ethical Standards

Conflict of Interest The authors declare that they have no conflict of interest.

References

Alt V, Cheung WH, Chow SK, Thormann U, Cheung EN, Lips KS, Schnettler R, Leung KS (2016) Bone formation and degradation behavior of nanocrystalline hydroxyapatite with or without collagen-type 1 in osteoporotic bone defects - an experimental study in osteoporotic goats. Injury 47:58–65

Bhatt RA, Rozental TD (2012) Bone graft substitutes. Hand Clin 28:457–468

Brandt J, Henning S, Michler G, Hein W, Bernstein A, Schulz M (2010) Nanocrystalline hydroxyapatite for bone repair: an animal study. J Mater Sci Mater Med 21:283–294

Campana V, Milano G, Pagano E, Barba M, Cicione C, Salonna G, Lattanzi W, Logroscino G (2014) Bone substitutes in orthopaedic surgery: from basic science to clinical practice. J Mater Sci Mater Med 25:2445–2461

Cassino PC, Rosseti LS, Ayala OI, Martines MA, Portugual LC, Oliveira CG, Silva IS, de Araujo R (2018) Potencial of different hydroxyapatites as biomaterials in the bone remodeling. Acta Cir Bras 33:816–823

Denry I, Kuhn LT (2015) Design and characterization of calcium phosphate ceramic scaffolds for bone tissue engineering. Dent Mater 32:43–53

Dimitriou R, Mataliotakis GI, Angoules AG, Kanakaris NK, Giannoudis PV (2011) Complications following autologous bone graft harvesting from the iliac crest and using the RIA: a systematic review. Injury 42:3–15

Dorozhkin SV (2010) Bioceramics of calcium thophosphates. Biomaterials 31:1465–1485

Fernandes KR, Magri AMP, Kido HW, Ueno F, Assis L, Fernandes KPS, Mesquita-Ferrari RA, Martins VC, Plepis AM, Renno ACM (2017) Characterization and biological evaluation of the introduction of PLGA into biosilicate®. J Biomed Mater Res B Appl Biomater 05:1063–1074

Fernandes KR, Parisi JR, Magri AMP, Kido HW, Gabbai-Armelin PR, Fortulan CA, Zanotto ED, Peitl O, Granito RN, Renno ACM (2019) Influence of the incorporation of marine spongin into a Biosilicate®: an in vitro study. J Mater Sci Mater Med 30:64

Gleeson JP, Plunkett NA, O'Brien FJ (2010) Addition of hydroxyapatite improves stiffness, interconnectivity and osteogenic potential of a highly porous collagen-based scaffold for bone tissue regeneration. Eur Cell Mater 20:218–230

Granito RN, Custódio MR, Rennó AC (2017) Natural marine sponges for bone tissue engineering: the state of art and future perspectives. J Biomed Mater Res B Appl Biomater 105:1717–1727

Green D, Howard D, Yang X, Kelly M, Oreffo RO (2003) Natural marine sponge fiber skeleton: a biomimetic scaffold for human osteoprogenitor cell attachment, growth, and differentiation. Tissue Eng 9:1159–1166

Guerado E, Caso E (2017) Challenges of bone tissue engineering in orthopaedic patients. World J Orthop 8:87–98

Haach LCA, Purquerio BM, Silva NF Jr, Gaspar AM, Fortulan CA (2014) Comparison of two composites developed to be used as bone replacement–PMMA/Bioglass 45S5® Microfiber and PMMA/Hydroxyapatite. Bioceram Dev Appl 4:071

Iwatsubo T, Kishi R, Miura T, Ohzono T, Yamaguchi T (2015) Formation of hydroxyapatite skeletal materials from hydrogel matrices via artificial biomineralization. J Phys Chem B 119:8793–8799

Junqua S, Robert L, Garrone R, Pavans de Ceccatty M, Vacelet J (1974) Biochemical and morphological studies on collagens of horny sponges Ircinia filaments compared to spongines. Connect Tissue Res 2:193–203

Komori T (2017) Roles of Runx2 in skeletal development. Adv Exp Med Biol 962:83–93

Lin K, Zhang D, Macedo MH, Cui W, Sarmento B, Shen G (2018) Advanced collagen-based biomaterials for regenerative biomedicine. Adv Funct Mater. https://doi.org/10.1002/adfm.201804943

Liu WC, Chen S, Zheng L, Qin L (2017) Angiogenesis assays for the evaluation of angiogenic properties of orthopaedic biomaterials - a general review. Adv Healthc Mater 6

Lopez-Heredia MA, Sa Y, Salmon P, de Wijn JR, Wolke JG, Jansen J (2012) A. Bulk properties and bioactivity assessment of porous polymethylmethacrylate cement loaded with calcium phosphates under simulated physiological conditions. Acta Biomater 8:3120–3127

Magri AM, Fernandes KR, Assis L, Mendes NA, da Silva Santos AL, de Oliveira DE, Rennó AC (2015) Photobiomodulation and bone healing in diabetic rats: evaluation of bone response using a tibial defect experimental model. Lasers Med Sci 30:1949–1957

Matassi F, Nistri L, Chicon Paez D, Innocenti M (2011) New biomaterials for bone regeneration. Clin Cases Miner Bone Metab 8:21–24

Mishra R, Bishop T, Valerio IL, Fisher JP, Dean D (2016) The potential impact of bone tissue engineering in the clinic. Regen Med 11:571–587

Oryan A, Alidadi S, Moshiri A, Maffulli N (2014) Bone regenerative medicine: classic options, novel strategies, and future directions. J Orthop Surg Res 9:18

Pang KM, Lee JK, Seo YK, Kim SM, Kim MJ, Lee JH (2015) Biologic properties of nano-hydroxyapatite: an in vivo study of calvarial defects, ectopic bone formation and bone implantation. Biomed Mater Eng 25:25–38

Parfitt AM (1988) Bone histomorphometry: standardization of nomenclature, symbols and units. Summary of proposed system. Bone Miner 4:1–5

Parisi JR, Fernandes KR, Avanzi IR, Dorileo BP, Santana AF, Andrade AL, Gabbai-Armelin PR, Fortulan CA, Trichês ES, Granito RN, Renno ACM (2019) Incorporation of collagen from marine sponges (spongin) into hydroxyapatite samples: characterization and in vitro biological evaluation. Mar Biotechnol 21:30–37

Parizi AM, Oryan A, Shafiei-Sarvestani Z, Bigham-Sadegh A (2013) Effectiveness of synthetic hydroxyapatite versus Persian Gulf coral in an animal model of long bone defect reconstruction. J Orthop Traumatol 14:259–268

Pek YS, Gao S, Arshad MS, Leck KJ, Ying JY (2008) Porous collagen-apatite nanocomposite foams as bone regeneration scaffolds. Biomaterials 29:4300–4305

Pozzolini M, Scarfì S, Gallus L, Castellano M, Vicini S, Cortese K, Gagliani MC, Bertolino M, Costa G, Giovine M (2018) Production, characterization and biocompatibility evaluation of collagen membranes derived from marine sponge *Chondrosia reniformis* Nardo, 1847. Mar Drugs 16:111

Raucci MG, Giugliano D, Alvarez-Perez MA, Ambrosio L (2015) Effects on growth and osteogenic differentiation of mesenchymal stem cells by the strontium-added sol–gel hydroxyapatite gel materials. J Mater Sci Mater Med 26:90

Sarkar SK, Lee BT (2015) Hard tissue regeneration using bone substitutes: an update on innovations in materials. Korean J Intern Med 30:279–293

Scarano A, Lorusso F, Staiti G, Sinjari B, Tampieri A, Mortellaro C (2017) *Sinus* augmentation with biomimetic nanostructured matrix: tomographic, radiological, histological and histomorphometrical results after 6 months in humans. Front Physiol 8:565

Siddiqui HA, Pickering KL, Mucalo MR (2018) A review on the use of hydroxyapatite-carbonaceous structure composites in bone replacement materials for strengthening purposes. Materials (Basel) 11:1813

Silva TH, Moreira-Silva J, Marques AL, Domingues A, Bayon Y, Reis RL (2014) Marine origin collagens and its potential applications. Mar Drugs 12:5881–5901

Smith JO, Aarvold A, Tayton ER, Dunlop DG, Oreffo RO (2011) Skeletal tissue regeneration: current approaches, challenges, and novel reconstructive strategies for an aging population. Tissue Eng B Rev 17:307–320

Sousa THS, Fortulan CA, Antunes ES, Purquerio BM (2019) Concept of a bioactive implant with functional gradient structure. Key Eng Mater 396:221–224

Swatschek D, Schatton W, Kellermann J, Müller WE, Kreuter J (2002) Marine sponge collagen: isolation, characterization and effects on the skin parameters surface-pH, moisture and sebum. Eur J Pharm Biopharm 53:107–113

Thorwarth M, Schultze-Mosgau S, Kessler P, Wiltfang J, Schlegel KA (2005) Bone regeneration in osseous defects using a resorbable nanoparticular hydroxyapatite. J Oral Maxillofac Surg 63:1626–1633

Walsh DP, Raftery RM, Chen G, Heise A, O'Brien FJ, Cryan SA (2019) Rapid healing of a critical-sized bone defect using a collagen-hydroxyapatite scaffold to facilitate low dose, combinatorial growth factor delivery. J Tissue Eng Regen Med 13:1843–1853

Wang W, Yeung K (2017) Bone grafts and biomaterials substitutes for bone defect repair: a review. Bioact Mater 2:224–247

Wang H, Li Y, Zuo Y, Li J, Ma S, Cheng L (2007) Biocompatibility and osteogenesis of biomimetic nano-hydroxyapatite/polyamide composite scaffolds for bone tissue engineering. Biomaterials 28:3338–3348

Wang B, Dong J, Zhou X, Lee KJ, Huang R, Zhang S, Liu Y (2009) Nucleosides from the marine sponge Haliclona sp. Z Naturforsch 64:143–148

Wei X, Egawa S, Matsumoto R, Yasuda H, Hirai K, Yoshii T, Okawa A, Nakajima T, Sotome S (2018) Augmentation of fracture healing by hydroxyapatite/collagen paste and bone morphogenetic protein-2 evaluated using a rat femur osteotomy model. J Orthop Res 36: 129–137

Zhang Z, Li Z, Zhang C, Liu J, Bai Y, Li S, Zhang C (2018) Biomimetic intrafibrillar mineralized collagen promotes bone regeneration via activation of the Wnt signaling pathway. Int J Nanomedicine 13: 7503–7516